Elsevier Editorial System(tm) for Biochimie
Manuscript Draft

Manuscript Number: BIOCHI-D-08-00142

Title: Palm tree Roystonea regia peroxidase: a plant peroxidase with unusually high stability

Article Type: Research Paper

Section/Category: Regular issue

Keywords: Palm peroxidase; Protein stability; Thermodynamics; Differential scanning calorimetry; Circular dichroism

Corresponding Author: Dr. Valery L. Shnyrov,

Corresponding Author's Institution: Universidade de Salamanca

First Author: Laura S Zamorano

Order of Authors: Laura S Zamorano; David G Pina, PhD; Juan B Arellano, PhD; Sergey Bursakov, PhD; Andrey P Zhadan, PhD; Juan J Calvete, PhD; Libia Sanz; Peter R Nielsen; Enrique Villar, PhD, Professor; Olga Gavel, PhD; Manuel G Roig, PhD; Leandra Watanabe, PhD; Igor Polikarpov, PhD; Valery L. Shnyrov

Manuscript Region of Origin: SPAIN

Abstract: The structural stability of a peroxidase, a dimeric protein from royal palm tree (Roystonea regia) leaves, has been characterized by high-sensitivity differential scanning calorimetry, circular dichroism, steady-state tryptophan fluorescence and analytical ultracentifugation under different solvent conditions. It is shown that the thermal and chemical (using guanidine hydrochloride (Gdn-HCl)) folding/unfolding of royal palm tree peroxidase (RPTP) at pH 7 is a reversible process involving a highly cooperative transition between the folded dimer and unfolded monomers, with a free stabilization energy of about 23 kcal per mol of monomer at 25 °C. The structural stability of RPTP is pH-dependent. At pH 3, where ion pairs have disappeared due to protonation, the thermally induced denaturation of RPTP is irreversible and strongly dependent upon the scan rate, suggesting that this process is under kinetic control. Moreover, thermally induced transitions at this pH value are dependent on the protein concentration, allowing it to be concluded

that in solution RPTP behaves as dimer, which undergoes thermal denaturation coupled with dissociation. Analysis of the kinetic parameters of RPTP denaturation at pH 3 was accomplished on the basis of the simple kinetic scheme N-k->D , where k is a first-order kinetic constant that changes with temperature, as given by the Arrhenius equation; N is the native state, and D is the denatured state, and thermodynamic information was obtained by extrapolation of the kinetic transition parameters to an infinite heating rate. Obtained in this way, the value of RPTP stability at 25 °C is ca. 8 kcal per mole of monomer lower than at pH 7. In all probability, this quantity reflects the contribution of ion pair interactions to the structural stability of RPTP. From a comparison of the stability of RPTP with other plant peroxidases it is proposed that the mechanism responsible for the unusually high stability of RPTP, which enhances its potential use for biotechnological purposes, is its dimerization.

Suggested Reviewers: Lev Weiner
lev.weiner@weizmann.ac.il
Very high level spesialist in the protein biochemistry and biophysics

Krassimira Idakieva
idakieva@orgchm.bas.bg
High level specialist in the calorimetry and spectroscopy of proteins

Dmitrii Levitsky
Levitsky@inbi.ras.ru
International level specialist in the biochemistry and biophysics of proiteins

Vladimir Uversky
vuversky@iupui.edu
One of the best expert in physico-chemistry of proteins

Opposed Reviewers:

Abstract

The structural stability of a peroxidase, a dimeric protein from royal palm tree (*Roystonea regia*) leaves, has been characterized by high-sensitivity differential scanning calorimetry, circular dichroism, steady-state tryptophan fluorescence and analytical ultracentifugation under different solvent conditions. It is shown that the thermal and chemical (using guanidine hydrochloride (Gdn-HCl)) folding/unfolding of royal palm tree peroxidase (RPTP) at pH 7 is a reversible process involving a highly cooperative transition between the folded dimer and unfolded monomers, with a free stabilization energy of about 23 kcal per mol of monomer at 25 °C. The structural stability of RPTP is pH-dependent. At pH 3, where ion pairs have disappeared due to protonation, the thermally induced denaturation of RPTP is irreversible and strongly dependent upon the scan rate, suggesting that this process is under kinetic control. Moreover, thermally induced transitions at this pH value are dependent on the protein concentration, allowing it to be concluded that in solution RPTP behaves as dimer, which undergoes thermal denaturation coupled with dissociation. Analysis of the kinetic parameters of RPTP denaturation at pH 3 was accomplished on the basis of the simple kinetic scheme $N \overset{k}{\rightarrow} D$, where k is a first-order kinetic constant that changes with temperature, as given by the Arrhenius equation; N is the native state, and D is the denatured state, and thermodynamic information was obtained by extrapolation of the kinetic transition parameters to an infinite heating rate. Obtained in this way, the value of RPTP stability at 25 °C is ca. 8 kcal per mole of monomer lower than at pH 7. In all probability, this quantity reflects the contribution of ion pair interactions to the structural stability of RPTP. From a comparison of the stability of RPTP with other plant peroxidases it is proposed that the mechanism responsible for the unusually high stability of RPTP, which enhances its potential use for biotechnological purposes, is its dimerization.

Author Agreement

All authors of the paper entitled “Palm tree *Roystonea regia* peroxidase: a plant peroxidase with unusually high stability” agree to send the manuscript for consideration by *Biochimie*. Material submitted is original and all authors are in agreement to have the article published.

On behalf of all co-authors of the manuscript,
Prof. Valery L. SHNYROV

*** Cover Letter**

Dear Editor,

Please find enclosed manuscript of our paper entitled "Palm tree *Roystonea regia* peroxidase: a plant peroxidase with unusually high stability" that I am sending you for consideration by **BIOCHIMIE**.

Sincerely yours,

Dr. Valery L. Shnyrov

Palm tree *Roystonea regia* peroxidase: a plant peroxidase with unusually high stability

Laura S. Zamorano [a], David G. Pina [b,1], Juan B. Arellano [c], Sergey Bursakov [d], Andrey P. Zhadan [e], Juan J. Calvete [f], Libia Sanz [f], Peter R. Nielsen [g,2], Enrique Villar [h], Olga Gavel [d], Manuel G. Roig [a], Leandra Watanabe[i], Igor Polikarpov [i], Valery L. Shnyrov [h,*]

[a] *Departamento de Química Física, Facultad de Ciencias Químicas, Universidad de Salamanca, 37008 Salamanca, Spain*

[b] *Department of Chemistry, University of Cambridge,Cambridge CB2 1EW, UK*

[c] *Instituto de Recursos Naturales y Agrobiologia (IRNASA-CSIC), Apdo. 257, 37071 Salamanca, Spain*

[d] *REQUIMTE, Departamento de Química, Centro de Química Fina e Biotecnologia, Faculdade de Ciências e Tecnologia, Universidade Nova de Lisboa, 2829-516 Caparica, Portugal*

[e] *Institute for Biological Instrumentation of the Russian Academy of Sciences, 142290 Pushchino, Moscow region, Russia*

[f] *Instituto de Biomedicina de Valencia, 46010 Valencia, Spain*

[g] *Department of Biochemistry, University of Cambridge, CB2 1GA, UK*

[h] *Departamento de Bioquímica y Biología Molecular, Universidad de Salamanca, 37007 Salamanca, Spain*

[i] *Instituto de Física de São Carlos, Universidade de São Paulo, São Carlos, SP CEP 13560-970, Brazil*

[1]*Present address:* Directorate-General for Research, European Commission, 1049 Brussels, Belgium.

[2]*Present address:* Department of Biochemistry, University of Leicester, Henry Wellcome Building, Lancaster Road, Leicester LE1 9HN, UK

Abbreviations: RPTP, royal palm tree -*Roystonea regia*- peroxidase; Gdn-HCl, guanidine hydrochloride; CD, circular dichroism; DSC, differential scanning calorimetry.

* Corresponding author. Tel.: +34 92 329 4465; fax: +34 92 329 4579.

E-mail address: shnyrov@usal.es (V.L. Shnyrov).

Abstract

The structural stability of a peroxidase, a dimeric protein from royal palm tree (*Roystonea regia*) leaves, has been characterized by high-sensitivity differential scanning calorimetry, circular dichroism, steady-state tryptophan fluorescence and analytical ultracentifugation under different solvent conditions. It is shown that the thermal and chemical (using guanidine hydrochloride (Gdn-HCl)) folding/unfolding of royal palm tree peroxidase (RPTP) at pH 7 is a reversible process involving a highly cooperative transition between the folded dimer and unfolded monomers, with a free stabilization energy of about 23 kcal per mol of monomer at 25 °C. The structural stability of RPTP is pH-dependent. At pH 3, where ion pairs have disappeared due to protonation, the thermally induced denaturation of RPTP is irreversible and strongly dependent upon the scan rate, suggesting that this process is under kinetic control. Moreover, thermally induced transitions at this pH value are dependent on the protein concentration, allowing it to be concluded that in solution RPTP behaves as dimer, which undergoes thermal denaturation coupled with dissociation. Analysis of the kinetic parameters of RPTP denaturation at pH 3 was accomplished on the basis of the simple kinetic scheme $N \overset{k}{\rightarrow} D$, where k is a first-order kinetic constant that changes with temperature, as given by the Arrhenius equation; N is the native state, and D is the denatured state, and thermodynamic information was obtained by extrapolation of the kinetic transition parameters to an infinite heating rate. Obtained in this way, the value of RPTP stability at 25 °C is ca. 8 kcal per mole of monomer lower than at pH 7. In all probability, this quantity reflects the contribution of ion pair interactions to the structural stability of RPTP. From a comparison of the stability of RPTP with other

plant peroxidases it is proposed that the mechanism responsible for the unusually high stability of RPTP, which enhances its potential use for biotechnological purposes, is its dimerization.

Key words: Palm peroxidase; Protein stability; Thermodynamics; Differential scanning calorimetry; Circular dichroism; Fluorescence; Analytical ultracentrifugation.

---

1. Introduction

Peroxidases (EC 1.11.1.7; donor: hydrogen peroxide oxido-reductase) are enzymes whose main function is to catalyze the conversion of hydrogen peroxide to water in the oxidation of a large number of substrates. However, such enzymes participate in many other reactions of biological significance, such as cell wall formation, lignification, suberization, auxin catabolism, defense, stress, developmentally related processes, protection of tissues from pathogenic microorganisms, etc [1]. Several peroxidases have been isolated, sequenced and characterized. They have essentially been classified in three classes on the basis of their amino acid sequence homology and metal ion-binding capabilities (class I, intracellular prokaryotic peroxidases; class II, extracellular fungal peroxidases, and class III, plant secretory peroxidases, in which RPTP is included). All class III peroxidases possess two calcium ions, an N-terminal signal peptide for excretion, and four disulfide bridges [2, 3].

Over time, peroxidases have attracted industrial attention. They now enjoy widespread use as catalysts for phenolic resin synthesis [4,5]; as indicators for food processing and diagnostic reagents [6,7], and as additives for bioremediation, especially for the removal of phenols, aromatic amines, and dyes from polluted water, etc [8, 9]. Modern applications of peroxidases include the production of conducting polymers, which have been of special interest in recent years [10]. Polyaniline is one such compound that can be used in lightweight organic batteries, in microelectronics, in optical displays, in anticorrosive protection, in bioanalysis as a sensor element, etc [11,12]. The synthesis of polyaniline can occur in the presence of peroxidase, hydrogen peroxide as a reducing substrate, and sulfonated polystyrene and poly(vinyl-phosphonic

acid) as polymeric templates [13] at acidic pH values (below pH 4.0). Thus, development of this and other biotechnological processes necessarily involves the characterization of the stability of peroxidases and their ability to be used under non-physiological conditions.

As with many enzymes, poor thermal and environmental stability limits the large-scale use of catalysis by peroxidases. This is particularly true in bioremediation and polyelectrolyte synthesis. Accordingly, the identification of highly stable and active peroxidases should be the first step in the development of a catalyst with broad commercial and environmental appeal. Recently, a peroxidase from royal palm tree (*Roystonea regia*) leaves (RPTP) has been isolated and partially characterized [14,15]). The substrate specificity of RPTP is similar to that of other plant peroxidases [14,16]. However, as shown in the present study, RPTP seems to have a very high stability; similar to that found in thermophilic microbial enzymes. This makes this peroxidase an intriguing catalyst for commercial and environmental applications. In the present study, different independent methods, such as differential scanning calorimetry (DSC), circular dichroism (CD), intrinsic fluorescence, and analytical centrifugation, were used to determine the structural stability of RPTP as a function of temperature, the protein concentration, the temperature scan rate, pH, and the chemical denaturant (Gdn-HCl) concentration.

2. Materials and methods

2.1. Materials

Analytical or extra-pure grade polyethyleneglycol (PEG), guaiacol (2-methoxyphenol), ammonium sulfate, sodium phosphate and Tris-HCl were purchased from Sigma Chemical Co. and were used without further purification. H_2O_2 was from Merck

(Darmstadt, Germany). Superdex-200 columns and Phenyl-Sepharose CL-4B were from GE Healthcare Bio-Sciences AB (Uppsala, Sweden). Toyopearl DEAE-650 M was purchased from the Tosoh Corporation (Tokyo, Japan). Cellulose membrane tubing for dialysis (avg. flat width 3.0 in.) was purchased from Sigma Chemical Co.; slide-A-lyzer dialysis cassettes (extra-strength, 3-12 mL capacity, 10.000 MWCO) were from Pierce Biotechnology, Inc. (Rockford, IL), and centrifuge filter devices (Amicon Ultra Cellulose 10.000 MWCO, 15 mL capacity) were from Millipore Corp. (Billerica, MA). All other reagents were of the highest purity available. The water used for preparing the solutions was double-distilled and then subjected to a de-ionisation process.

2.2. Protein Preparation

RPTP was purified from royal palm tree (*Roystonea regia*) leaves as described elsewhere [15]. A mass of 835 g of seven-year-old royal palm leaves was milled and homogenized in 3.34 L of water for 22-24 h at room temperature. The excess material was removed by vacuum filtration, followed by centrifugation at 10,000 *g*, 4-5 ºC, for 15 min in a Refrigerated Sorvall RC 5B Superspeed Centrifuge (Thermo Fisher Scientific, Inc., Waltham, MA). Pigments were extracted by phase separation over 20-22 h at 4-5 ºC after the addition to the supernatant of solid PEG (10,000 MW) up to 14 % (w/v) and solid $(NH_4)_2SO_4$ (w/v) up to 10 % (w/v). Two phases were formed after the addition of $(NH_4)_2SO_4$: an upper, dark-red polymer phase, consisting of pigments, phenols, polyphenols, oxidized phenols and PEG, and a lower, yellow aqueous phase containing peroxidase. Each phase contained 50 % of the initial volume. These phases were separated by decantation and the phase containing peroxidase activity was centrifuged at 10,000 *g* at 4-5 ºC for 15 min. The clear supernatant containing

peroxidase activity was titrated with $(NH_4)_2SO_4$ until a conductivity value of 326 mS cm^{-1} was reached, after which it was loaded onto a Phenyl-Sepharose column (1.5×50 cm) equilibrated with 100 mM phosphate buffer, pH 6.5, and 1.7 M $(NH_4)_2SO_4$ with the same conductivity as that of the sample. The enzyme was eluted with 100 mM phosphate buffer, pH 6.5, plus 0.2 M $(NH_4)_2SO_4$ at a flow rate of 1 mL min^{-1}. Fractions of 15 mL were collected and those showing peroxidase activity were dialyzed against 5 mM Tris-HCl buffer, pH 8.3, for 24 h with constant stirring at 4-5 ºC. The dialyzed sample was 3-fold membrane-concentrated (Amicon, cut-off 10 kDa) in an Allegra 21R centrifuge (Beckman Coulter, Inc. Fullerton, CA) and loaded onto a DEAE-Toyopearl 650 column (1×30 cm) equilibrated with 5 mM Tris-HCl buffer, pH 8.3. The sample was eluted with a linear gradient of increasing NaCl concentration from 0 to 300 mM at a flow rate of 1 mL min^{-1}. The fractions with peroxidase activity were collected, 8-fold membrane-concentrated (Amicon, cut-off 10 kDa), and loaded onto a Superdex-200 column equilibrated with 5 mM Tris-HCl buffer, pH 8.3. Elution was carried out at a flow rate of 0.5 mL min^{-1}. Finally, the fractions containing highly pure peroxidase were dialyzed against distilled water and freeze-dried.

The purity of the RPTP was determined by SDS-PAGE, as described by Fairbanks et al. [17], on a Bio-Rad minigel device, using a flat block with a 15 % polyacrylamide concentration; by gel-filtration, performed using a Superdex 200 10/30 HR column connected to an ÄKTA-purifier system (GE Healthcare Bio-Sciences AB, Uppsala, Sweden); by UV-visible spectrophotometry ($RZ \equiv A_{403}/A_{280}$ = 2.8-3.0), and by MALDI-TOF mass spectrometry using an Applied Biosystems Voyager-DE-Pro mass spectrometer operating in linear mode. Analytical isoelectrofocusing was performed on a Mini IEF cell model 111 (Bio-Rad Laboratories, Hercules, CA) using Ampholine PAG-plates, pH 3.5-9.5 (GE Healthcare Bio-Sciences AB, Upsala, Sweden).

Electrophoretic conditions and Coomassie brilliant blue R-250 staining were as recommended by the manufacturer. The standards used were from a broad-range p*I* calibration kit (pH 4.45-9.6) from Bio-Rad Laboratories (Hercules, CA).

Protein concentrations were determined spectrophotometrically, using the experimentally determined extinction coefficient value at 403 nm for the protein monomer of 59.1 ± 0.6 $mM^{-1}cm^{-1}$.

Peroxidase activity toward guaiacol was measured spectrophotometrically at 25 °C. An aliquot of enzyme solution was added to a 1-cm spectral cuvette containing 18.1 mM guaiacol and 4.9 mM H_2O_2 in 20 mM sodium phosphate buffer, pH 6.0, in a final volume of 2 mL. The rate of change in absorbance due to substrate oxidation was monitored at 470 nm. Peroxidase activities were calculated using a molar absorption coefficient of 5200 $M^{-1}cm^{-1}$ at 470 nm for the guaiacol oxidation product [18].

In titration experiments, pH values were adjusted by means of a polyethylene rod moistened with either 0.1 M HCl or 0.1 M NaOH.

2.3. Analytical Ultracentrifugation

Equilibrium sedimentation experiments were performed at 25 °C in a Beckman Optima XL-I analytical ultracentrifuge, using double-sector cells with 1.2-cm thick charcoal-filled Epon centerpieces in an An60-Ti rotor. The RPTP concentration of 1 mg mL^{-1} in 20 mM citrate buffer, pH 3.0, in the presence of 6 M GuHCl was used, since under these conditions the protein is fully denatured and hence monomeric. Cells were loaded with 100 µl of protein and 110 µl buffer aliquots. Absorbance data were acquired at 275 nm. Samples were centrifuged at 24,000 and 32,000 rpm, and equilibrium was

confirmed by the overlay of consecutive scans. The molecular masses of the samples were determined by non-linear fitting using SEDPHAT [19].

Sedimentation velocity experiments were carried out under the same instrumental conditions described above, at 45000 rpm. Protein solutions of 1.0 and 2.5 mg mL^{-1} were dialyzed against buffer containing 20 mM HEPES buffer, at pH 7.0, or 20 mM citrate buffer, at pH 3.0. Aliquots of protein solution of 0.38 mL and 0.4 mL of the respective dialysis buffers were loaded into the sample and reference cells. Sedimentation was monitored for 3 hours by acquiring absorbance data at 280 nm at time intervals of 4 min, with separate runs for each pH. Using the SEDFIT program [19], the sedimentation velocity data were fitted to a superposition of discreet Lamm equation solutions, generating a continuous distribution of sedimentation coefficients C(S) after regularization (F-ratio 0.95) [20]. Molecular masses were calculated from these data by means of the Svedberg equation.

2.4. Differential Scanning Calorimetry

Calorimetry scans were performed on a MicroCal MC-2D differential scanning microcalorimeter (MicroCal Inc., Northampton, MA) with cell volumes of 1.22 mL as described previously [21,22]. All solutions were degassed by stirring under a vacuum prior to scanning. An overpressure of 2 atm of dry nitrogen was always kept over the liquids in the cells throughout the scans. The reversibility of the thermal transitions was checked by examining the reproducibility of the calorimetric trace in a second heating of the sample immediately after cooling from the first scan. The molar excess heat capacity curves obtained by normalization with the protein concentrations and volume of the calorimeter cell were smoothed and plotted using the Windows-based software

package (ORIGIN) supplied by MicroCal Inc. (Northampton, MA). Analysis of the data was accomplished on the basis of:

1) The two-state folding/unfolding reaction coupled with the oligomerization model. This model corresponds to a situation in which the oligomeric protein made up of identical subunits obeys the following equilibrium:

$$\frac{1}{n}N_n \overset{K}{\longleftrightarrow} U \tag{1}$$

$$K = \frac{[U]}{[N_n]^{1/n}} \tag{2}$$

where $[N_n]$ and $[U]$ represent the concentration of folded oligomer and unfolded monomer, respectively, and n is the number of dissociable subunits. If α is the fraction of protein in the denatured state and (1- α) is the fraction of protein in the native state, the equilibrium constant can be written as:

$$K = n^{1/n} \cdot C_t^{(n-1)/n} \frac{\alpha}{(1-\alpha)^{1/n}} \tag{3}$$

where C_t is total molar monomer concentration.

Using Eq. (3) and the expressions for enthalpy change, which is,

$$\left[\frac{d\ln K}{dT}\right]_p = \frac{\Delta H(T)}{RT^2} = \frac{\Delta H_{1/2} + \Delta C_p \cdot (T - T_{1/2})}{RT^2} \quad , \tag{4}$$

it is easy to express K as function of temperature:

$$K(T) = \frac{1}{2}\left(\frac{n}{2}\right)^{1/n} C_t^{(n-1)/n} \exp\left[-\frac{\Delta H_{1/2}}{R}\left(\frac{1}{T} - \frac{1}{T_{1/2}}\right) - \frac{\Delta C_p}{R}\left(1 - \frac{T_{1/2}}{T} + \ln\frac{T_{1/2}}{T}\right)\right] \tag{5}$$

where R is the gas constant, $\Delta H_{1/2}$ and ΔC_p are the changes in the enthalpy and heat capacity upon unfolding, respectively, and $T_{1/2}$ is temperature value, where α = 0.5.

Once $K(T)$ is known, then $\alpha(T)$ can be solved numerically from Eq. (5) and the excess heat capacity function $\langle \Delta C_p \rangle$, which is simply the temperature derivative of the average excess enthalpy, can be written as:

$$\left\langle \Delta C_p \right\rangle = \frac{d\left\langle \Delta H \right\rangle}{dT} = \frac{d\alpha(T)}{dT} \cdot \Delta H_{1/2} + \alpha \cdot \Delta C_p \qquad (6)$$

The above equations were used to fit the data and to obtain the best estimates for $\Delta H_{1/2}$, ΔC_p and $T_{1/2}$.

2) the simple two-state irreversible model, $N_2 \xrightarrow{k} D$, where N_2 is the native dimer, D is the denatured monomer and k is the effective rate constant for the denaturation that changes with temperature, as given by the Arrhenius equation: $k = \exp[E_A(1/T^*-1/T)/R]$, where E_A is the energy of activation, and T^* is the temperature at which the rate constant equals 1 min^{-1}. In this case the excess heat capacity C_p^{ex} is given by the following equation [23]:

$$C_p^{ex} = \frac{1}{\nu}\Delta H \exp\left\{\frac{E_A}{R}\left(\frac{1}{T^*}-\frac{1}{T}\right)\right\} \times \exp\left\{-\frac{1}{\nu}\int_{T_o}^{T}\exp\left[\frac{E_A}{R}\left(\frac{1}{T^*}-\frac{1}{T}\right)\right]dT\right\} \qquad (7)$$

where $\nu = dT/dt$ (K/min) is a scan rate value and ΔH is the enthalpy difference between the denatured and native states.

2.5. Circular Dichroism

The far-UV CD spectra (190-250 nm) of RPTP were recorded on a Jasco-715 spectropolarimeter (JASCO Inc., Easton, MD), using a spectral band-pass of 2 nm and a cell path length of 1 mm. Protein concentrations of 0.1 to 0.2 mg/ml were used in these measurements. Four spectra were scanned for each sample at a scan rate of 50 nm min^{-1} and were then averaged. All spectra were background-corrected, smoothed, and converted to mean residue ellipticity $[\Theta] = 10\ M_{res}\ \Theta_{obs}\ l^{-1}\ p^{-1}$, where $M_{res} = 104.5$ is the mean residue molar mass calculated from the protein sequence; Θ_{obs} is the ellipticity

(degrees) measured at wavelength λ; *l* is the optical path-length of the cell (dm), and *p* is the protein concentration (mg/ml).

Thermal stability experiments were performed between 30 and 80 °C with a constant heating rate of 1 K min^{-1} using a Neslab RT-11 programmable water bath (Thermo Fisher Scientific, Inc., Waltham, MA), and were followed by continuous measurements of ellipticity at 222 nm. Denaturation curves were transformed into the fractional degree of denaturation by the following equation, using a non-linear least squares algorithm:

$$\theta = \theta_N \cdot (1-\alpha) + \theta_U \cdot \alpha \quad (8)$$

where $\theta_N = a_1 + a_2 \cdot x$ and $\theta_U = b_1 + b_2 \cdot x$ represent the mean values of ellipticity for the native and unfolded conformations, respectively, obtained by linear regression of pre- and post-transitional baselines; *x* is the variable parameter.

2.6. Intrinsic Fluorescence

Steady-state fluorescence measurements were performed on a Hitachi F-4010 spectrofluorimeter (Hitachi Co., Ltd. Tokyo, Japan). Excitation was performed at 296 nm (with excitation and emission slit widths of 5 nm). The fluorescence measurements of RPTP were carried out on protein solutions with an optical density of less than 0.2 at 280 nm to avoid the inner filter effect. All emission spectra were corrected for instrumental spectral sensitivity. Measurements of pH-dependent changes in protein fluorescence were performed by downward or upward titration of the protein solution from an initial pH of 7.0, adjusting by means of a polyethylene rod moistened with either 0.1 M HCl or 0.1 M NaOH. The temperature dependence of the fluorescence spectral characteristics was investigated using thermostatically-controlled water

circulating in a hollow brass cell-holder. Temperature in the sample cell was monitored with a thermocouple immersed in the cell under observation. The heating rate was 1.8 K min^{-1}, and spectra were collected at the desired temperatures over the entire temperature range. Melting curves were transformed into the fractional degree of denaturation, as in the case of the CD measurements.

3. Results and discussion

3.1. pH Dependence

It is known that both the structural stability and the enzymatic activity of peroxidases strongly depend on the pH of the solution [24-26] However, although plant peroxidases have been studied for many years, information about their pH-dependent behavior is still very limited. To choose the most suitable pH conditions for stability studies, here we measured the pH dependence of the enzymatic activity and tryptophan fluorescence of RPTP (Fig. 1).

RPTP is a highly stable enzyme over a broad pH-range -from pH 2 to13- with at least two steps in the enzymatic activity changes, with apparent pK_a values of about 4.4 and 8.9 (Fig. 1B), which do not coincide with the changes in the spectral parameters. Thus, one of the most useful parameters of the protein fluorescence spectrum -its maximum position (λ_{max}), which reflects the degree of accessibility of the chromophores to solvent molecules [27]- remains constant (variation in limits of ± 0.3 nm) within a pH-range from about 2.8 to 10.3. This implies that the accessibility of the RPTP tryptophan side chains to water molecules remains essentially invariant in this pH range. Furthermore, the fluorescence intensity did not change, indicating the absence of

changes in the fluorescence quenching properties of the tryptophan environment in this pH-range. Thus, the pH range from 3 up to 10, characterized by the absence of evident pH-dependent fluorescence changes, seems to be the correct range of choice for the physico-chemical characterization of RPTP. Acidification of the protein solution down to a pH of less than 2 caused a 3.2 nm red shift in the fluorescence spectrum, followed by a blue shift after pH 1.2, brought about by protein aggregation and a marked (more than 4-fold) increase in fluorescence intensity. These changes, together with changes in enzymatic activity, seem to reflect an acidic denaturation of RPTP. Increasing the pH to more than 10.8 resulted in a considerable (ca. 11 nm) red shift of the fluorescence spectrum, reflecting an increase in the polarity of the tryptophan side chain environment followed by a blue shift after pH 12.5, probably related to an aggregation that would preserve the complete hydration of tryptophan, and an insignificant increase in fluorescence intensity (only after pH 13). Comparison of these changes with the changes in enzymatic activity indicates that only the fluorescence intensity reflects protein denaturation, while the position of the fluorescence spectrum, reflecting the polarity of the tryptophan side chain environment, shows that polarity is not relevant for the enzymatic function of RPTP.

3.2. RPTP is a Homodimer in Solution

In our previous paper [15] it was reported that following the data of size exclusion chromatography, RPTP forms dimers in solution with an approximate molecular mass of 90 kDa while the molecular mass of the monomer (SDS-PAGE data) is ca. 50 kDa. To examine the oligomeric state of RPTP more accurately, velocity and equilibrium sedimentation experiments were performed.

Fig. 2A (see also Table 1) shows the normalized molar distribution of RPTP under different pH and protein concentrations, as a function of the sedimentation coefficient. RPTP samples at high (2.5 mg mL^{-1}) and low (0.8 mg mL^{-1}) concentrations were centrifuged in 20 mM HEPES, pH 7.0, and in 20 mM citrate buffer, pH 3.0. In all conditions, only one major species was observed to have a symmetrical distribution, with an average sedimentation coefficient of 6.2 ± 0.2 S, which corresponds to a molecular mass of 88.5 ± 4.9 kDa. Taking into account that the molecular weight of RPTP obtained by MALDI-TOF mass spectrometry was 44590 ± 8 Da, we propose that this peroxidase would exist as a dimer in solution. In fact, it should be taken into account that at pH 7, with a protein concentration of 2.5 mg mL^{-1}, nearly 2 % of the molecular population is observable, with a sedimentation coefficient of 9.9 ± 0.5 (molecular mass of 188.1 ± 10.3 kDa), suggesting that at neutral pH and at a high protein concentration a small amount of a tetrameric form of RPTP is being formed.

According to the circular dichroism data, RPTP loses its secondary structure in 6 M Gdn-HCl at pH 3.0 (data not shown). Owing to its random coiled state under these conditions, we performed equilibrium sedimentation measurements, which do not depend on the shape of the protein, to determine the molecular mass of protein. These equilibrium sedimentation experiments confirmed that under the experimental conditions employed neither the aggregation nor oligomerization of RPTP occurs in solution, although a slight deviation from ideality was found upon fitting the result to a single protein species. A molecular mass of 44.200 ± 2.2 kDa was obtained (Fig. 2B). The above allows an equilibrium ($N_2 \leftrightarrow 2U$) to be assumed between a dimer in the native state and a monomer in the unfolded (or denatured) state.

3.3. DSC

Fig. 3A (continuous line) shows the temperature dependence of the excess molar heat capacity of RPTP in 20 mM HEPES buffer at pH 7.0. To examine the reversibility of the heat denaturation, the second calorimetric scan was performed just after the cooling of the first one, and the recovery area of excess heat capacity due to the denaturation was measured. Despite this, owing to the aggregation that follows denaturation it is very difficult to observe the heat reversibility of proteins with a denaturation temperature close to 100 °C at neutral pH values. In the case of RPTP, the reversibility at pH 7 was very good: the recovery rate was more than 80% after the first heating up to 100 °C (Fig. 3A, dashed line). However, prolonged incubation of the samples at high temperature resulted in the appearance of an irreversible process. For example, after the incubation of RPTP at 105 °C or higher for longer than 5 min in repeated scans, approximately only 20% of the transitional enthalpy of the preceding scan was retained. Experiments performed at scanning rates of 0.35 and 1.4 K min^{-1} afforded practically the same denaturation profiles (data not shown), indicating the absence of kinetic effects at pH 7.0. Owing to the dimeric nature of RPTP, the stability of the native form is concentration-dependent (Fig. 3B). It may be seen that all transition peaks are skewed toward the low-temperature side of the transition, as expected for a transition coupled to dissociation, according to Eq. (1) [28,29]. Consequently, the temperature of the midpoint of the transition $T_{1/2}$ does not coincide with the temperature of the excess heat capacity maximum, T_m. For the calorimetric contours obtained for different protein concentrations in this work, the ratio of the van ‘t Hoff and calorimetric enthalpies, $\Delta H_{VH}/\Delta H(T_m)$, obtained at a temperature where α = 0.5, averaged 1.30±0.05, which is reasonably close to the value calculated using the expression:

$$\frac{\Delta H_{VH}}{\Delta H(T_m)} = \frac{2 \cdot n}{n+1} \qquad (9)$$

which is valid for the situation in which the unfolding of oligomeric proteins is coupled with their dissociation-unfolded monomers [29]: i.e., 1.333 for a dimer.

In a general coupling between the unfolding and dissociation processes, equilibrium thermodynamics predicted the following relationship between the total monomer concentration, A_t, and the unfolding temperature T_m [29,30]:

$$\ln A_t = \text{constant} - n\Delta H(T_m)\cdot(n-1)^{-1}\cdot R^{-1}\cdot T_m^{-1} \qquad (10)$$

The plot of ln A_t vs. T_m^{-1} (Fig. 4) yielded a straight line. The value of $\Delta H(T_m)$ obtained from the slope of this line is 192.3 ± 8.5 kcal mol^{-1}, very close to the values of the calorimetric enthalpy for RPTP (Table 2).

The experimental calorimetric data obtained at different RPTP concentrations were fitted individually to the two-state folding/unfolding oligomerization model according to Eq. (6). This fitting afforded excellent results for n = 2 (see lines through the data points in Fig. 3B), whereas a similar fitting for other n values was much poorer. The highest-likelihood values for the thermodynamic parameters obtained from the fittings are shown in Table 2.

All the above data allowed us to conclude that in solution at pH 7.0 RPTP behaves as a dimer that undergoes a two-state reversible thermal unfolding coupled with dissociation.

It was next considered of interest to investigate the denaturation of RPTP in the acid pH range, where ion pairs, which are known to be important for the stability of haeme-containing class III peroxidases [24], have disappeared due to protonation. This was done in order to estimate their influence in structural stabilization and also to compare the stability of RPTP with that of other plant peroxidases with a view to using this enzyme for the “green” synthesis, at acid pH, of polyelectrolyte complexes of polyaniline [10]. pH 3 is a very appropriate value for such ends because it is distant

from the pI of RPTP (5.3) and lies in the zone characterized by the absence of evident pH-dependent enzymatic and fluorescence changes.

The thermal denaturation of RPTP at pH 3.0 gave rise to well defined DSC transitions whose apparent T_m values were dependent on the temperature scan rate. This effect can be seen in Fig. 5, which shows the thermal transitions for RPTP at three scan rates. The thermal denaturation of RPTP under these experimental conditions was always calorimetrically irreversible since in a second heating of the enzyme solution no thermal effect was observed. All this clearly indicates that the observed thermal transitions characterize an irreversible, kinetically controlled process. Since RPTP is a dimeric protein, thermally induced denaturation should be accompanied by its dissociation into subunits (see the above results at pH 7.0), which should produce a concentration dependence of T_m [28,31,32]. In fact, the T_m and ΔH_{cal} values for the thermal denaturation of RPTP at pH 3.0 were found to be dependent on the protein concentration within the 0.5 – 2.4 mg mL^{-1} range (data not shown) and the ratio of the van 't Hoff and calorimetric enthalpies obtained at different concentrations and different scan rates averaged 1.4 ± 0.1, fairly close to the value calculated with Eq. (9), which is valid for the case when the denaturation of the dimer is coupled to its dissociation into monomers (see above). Accordingly, despite, a very small variation in the kinetic parameters of RPTP denaturation with concentration, in all the experiments performed at this pH we used the same concentration of protein to be sure that results obtained in different experiments would be concentration independent. Analysis of the DSC transitions under these conditions was accomplished on the basis of a simple two-state irreversible model $N_2 \overset{k}{\rightarrow} D$ (see Materials and Methods). It should be noted that a realistic model of protein denaturation in this case should include two steps: reversible unfolding and irreversible alteration of the unfolded state to produce the final denatured

state, which is unable to fold back to the native protein. This scheme, usually known as the Lumry-Eyring model [33] in case of dimeric proteins, can be depicted as: $N_2 \underset{k_{-1}}{\overset{k_1}{\leftrightarrow}} 2U \overset{k_d}{\rightarrow} D$, where N_2 is the native dimer, U is the unfolded monomer, D is the irreversibly denatured monomer, k_1 and k_{-1} are the rate constants for the forward and reverse unfolding process with concomitant dissociation, and k_d is the rate constant for the denaturation of the monomers. However, use of the whole Lumry-Eyring model for the quantitative description of thermally induced transitions is difficult because the corresponding system of differential equations does not have an analytical solution at varying temperatures. It is therefore necessary to evaluate simpler mathematical models that are particular cases of the whole Lumry-Eyring model. In the present work we used the model that includes only one irreversible step, assuming that monomer denaturation is rapid in comparison with the dissociation of the dimer and the association of monomers, t. e. $k_d \gg k_1$ and $k_d \gg k_{-1}$. This means that the thermally induced disruption of the quaternary structure of the dimer adheres kinetically to the "all-or-not" law: $N_2 \overset{k}{\rightarrow} D$ (see Materials and Methods).

The excess heat capacity functions obtained for RPTP in this case were analyzed by fitting the data to the two-state irreversible model -Eq. (7)- either individually or globally, using scan rate as an additional variable. The results of the fitting are shown in Fig. 5 (solid lines) and in Table 3. As can be seen, when fitting was carried out both separately on the individual experimental curves and simultaneously on all the curves, a good approximation was achieved. Attempts to include different irreversible models for RPTP denaturation - the Lumry-Eyring model, with a fast equilibrating first step, and the model that includes two consecutive irreversible steps [34,35] - did not improve the goodness of the fit, indicating that the two-state irreversible model is sufficient to

quantitatively describe the kinetics of RPTP denaturation. This conclusion was further confirmed by our spectral investigation on the thermal denaturation of this enzyme.

It is interesting to compare the kinetic parameters of RPTP stability with those of other peroxidases. In previous publications [21,25,36] we reported the results of a detailed investigation of the thermal denaturation of horseradish peroxidase isoenzyme *c* (HRP*c*), anionic peanut (*Arachis hypogaea* L.) peroxidase (aPrx) and peroxidase from the African oil palm tree *Elaeis guineensis* (AOPTP). It is clear that the thermostability of RPTP is substantially greater than that of HRP*c* and aPrx, and is practically the same as the stability of AOPTP. Thus, the T_m for RPTP at a scan rate of 60 K h^{-1} is 67.7 ± 0.2 °C while for aPrx this value is 39.4 ± 0.2 °C; for HRP*c* it is 60.2 ±0.2 °C and for AOPTP it is 72.3 ± 0.2 °C. In any case, the Arrhenius energy of activation for RPTP - 129.1 ± 0.8 kcal mol^{-1} - is the highest value in comparison not only with those of HRPc (38.2 ± 0.5 kcal mol^{-1}), aPrx (67.9 ± 0.5 kcal mol^{-1}) and AOPTP (103 ± 6 kcal mol^{-1}) but of all other plant peroxidases [37,38].

It is clear that equilibrium thermodynamics cannot be applied directly in the analysis of RPTP denaturation at pH 3 because of its kinetically controlled nature. However, it is possible to obtain some useful thermodynamic information upon extrapolation of the transition parameters to the infinite heating rate [39]. The thermodynamic parameters obtained for the thermal denaturation of RPTP at pH 3 are shown in Table 2.

Fig. 6 shows the theoretical curves, known as protein stability curves, for RPTP at pH 3 and 7 calculated with the Gibbs-Helmholtz equation [40]:

$$\Delta G^{o}(T) = \Delta H(T_{1/2}) \cdot (1 - T/T_{o}) - \Delta C_{p} \cdot [(T_{o} - T) + T \cdot \ln(T/T_{o})] \qquad (11)$$

where $\Delta G^{o}(T)$ is the standard free energy change, T_o is the temperature value at which $\Delta G^{o}(T)$ = 0, $\Delta H(T_{1/2})$ is the experimental transition enthalpy at $T_{1/2}$, and ΔC_p is the

difference in heat capacity between the native and denatured conformations, which was obtained from the slope of plot ΔH vs. T using data collected at different pH values in the pH range from 3 to 9 (data not shown), according to the Kirchoff equation:

$$\Delta C_p = d(\Delta H)/d(T) \quad (12)$$

The numerical value of ΔC_p for RPTP thus obtained was 2.4 ± 0.1 kcal K^{-1} mol^{-1}.

The stability of RPTP at 25 °C (pH 7) is 23.3 ± 0.1 kcal mol^{-1}, that seems very high because it is known that in biological processes energy is exchanged, as a rule, by portions of 4-8 kcal mol^{-1}, and hence the upper limit of the protein conformational stability should have the same value. The possible reason for this high stability is not clear.

It may be seen that at pH 3 the stability at 25 °C is ca. 8 kcal mol^{-1} lower and in all likelihood this quantity would reflect the contribution of ion-pair interactions in the structural stability of RPTP [41].

3.4. CD Experiments

Fig. 7A shows the far-UV CD spectra of RPTP at 0 and 7.1 M Gdn-HCl in 20 mM HEPES (pH 7.0) at 25 °C. The spectrum in the intact state exhibits a strong positive band, with a maximum at 194 nm and double minima at 208 and 222 nm, indicative of proteins with a high content of an α-helical structure. A detailed secondary structure analysis of the CD spectra was performed using the CDPro software package [42]. The experimental data in 190-240 nm range were subjected to treatment by three programs included in this software package -SELCON3, CDSSTR, and CONTINLL- using the SP43 (for intact proteins) and SDP48 (for denatured proteins) reference sets. The lowest root mean square deviation (RMSD) between the experimental data and the theoretical

curves produced by the programs with this reference set was obtained with CDSSTR, and hence the results obtained with SELCON3 and CONTINLL were omitted. The results of this analysis are given in Table 4. The values thus obtained for intact RPTP are typical of different heme peroxidases [43]. It should be noted here that the estimates for the β-sheet and β-turn are usually worse than the estimate for the α-helix because the intensities of the β structure elements are lower than those of the α-helix [44]. As can clearly be seen in Fig. 7A, secondary structure analysis is not feasible for the CD data acquired for the protein in the presence of Gdn-HCl because the absorption of Gu-HCl precludes measurements at wavelengths of less than 210 nm.

The Gdn-HCl-induced unfolding of RPTP (Fig. 7B) was monitored by changes in the ellipticity at 222 nm at 25 ^{o}C. The experimental data obtained at this temperature at pH 7.0 were analyzed with the same two-state folding/unfolding oligomerization model -Eq. (1)- that was used to fit the heat-induced unfolding of the RPTP monitored by DSC, because the refolding of RPTP revealed that the chemical denaturation by Gdn-HCl was a reversible process (data not shown). In this case, the dependence of the difference in free energy between the native and denatured conformations of RPTP was obtained using the classic thermodynamic equation:

$$\Delta G^{\circ} = -R\,T \ln K \qquad (13)$$

where ΔG^{o} refers to the Gibbs free energy change induced by the displacement of the equilibrium from the initial standard state (a hypothetical state in which the concentrations of both the dimer and monomer are 1 M) to its final equilibrium state, in which the concentrations of the dimer and monomer are governed by the equilibrium constant *K*, which was calculated according to Eq. (3). A plot of ΔG° *vs.* [Gdn-HCl] is shown in an inset in Fig. 7B (symbols) and was fitted (straight line) following the linear extrapolation method [45]:

$$\Delta G° = \Delta G°(H_2O) - m\,[\text{Gdn-HCl}] \qquad (14)$$

where $\Delta G°(H_2O)$ is the Gibbs energy change in the absence of Gdn-HCl, and m reflects the variation of the dependence of the free energy change upon denaturation, $\Delta G°$, on the Gdn-HCl concentration.

As shown in Fig. 7B (inset), this model offers a good explanation for the RPTP denaturation data obtained by CD (with a linear correlation coefficient of 0.9987). The m value is 2.94 ± 0.05 kcal mol^{-1} $[\text{Gdn-HCl}]^{-1}$ (slightly less than that observed for other proteins of similar molecular weight [46]). The conformational stabilities of RPTP, $\Delta G°(H_2O)$, at 25 °C is 23.3 ± 0.3 kcal mol^{-1} (see circle in Fig. 6), in close agreement with the ΔG value extrapolated from the thermodynamic parameters obtained from the heat-induced unfolding experiments monitored by DSC (Table 2).

Accordingly, the results of both the chemical and the thermal denaturation experiments are in agreement with a two-state model in which the population of folded monomers throughout the transition is negligible, and only dimers and unfolding monomers are significantly populated.

The CD spectra of intact and thermally denatured RPTP at pH 3.0 are shown in Fig. 7C. The fractions of secondary structure elements obtained following the CDSSTR method (see above) are given in Table 4. Upon heating the RPTP up to the denaturation temperature, the shape of the spectrum changed, pointing to an increase in the unordered structure, mainly at the expense of the α-helical structure (see Table 4). The increase in the quantity of β-strands that also occurred in denatured RPTP indicates that this form of the enzyme undergoes some aggregation, most probably with an intramolecular character, because we failed to detect an increase in turbidity in the denaturation process.

The thermal denaturation of RPTP was monitored by following the changes in molar ellipticity at 222 nm since at this wavelength the changes in ellipticity are significant upon enzyme denaturation. With increasing temperature (Fig. 7D), an irreversible cooperative transition to the denatured state occurred, which was analyzed by using a non-linear least squares fitting to Eq. (15) (see line through the data points):

$$F_{\mathrm{d}} = 1 - \exp\left\{ -\frac{1}{\nu} \int_{T_{\mathrm{o}}}^{T} \exp\left[\frac{E_{\mathrm{A}}}{R} \left(\frac{1}{T^*} - \frac{1}{T} \right) \right] dT \right\} \qquad (15)$$

where F_{d} refers to the denatured fraction [23]. This fitting affords the T^* parameter and the activation energy for RPTP. These values are 343.5±1.7 K and 124.1 ± 3.1 kcal mol^{-1}, respectively, which are similar to those observed for the same parameters obtained by DSC (Table 3).

Fluorescence Experiments. Environmental changes in aromatic side chains resulting from conformational changes in the tertiary structure of proteins were measured by intrinsic fluorescence spectroscopy. Fig. 7E shows the fluorescence spectra of intact (solid line) and thermally denatured (dashed line) RPTP at pH 3.0, excited at 296 nm. The fluorescence emission of the intact RPTP has a very low quantum yield due to energy transfer to the heme which, as can be seen in Fig. 7E, essentially increases in the denatured enzyme owing to a change in the relative orientation or distance between the heme and the tryptophan residue(s) [47]. In view of these results, we used the changes in fluorescence intensity to analyze the effect of heating on the RPTP denaturation process. On increasing temperature (Fig. 7F), an irreversible cooperative transition to the denatured state occurred, which was analyzed by non-linear least squares fitting to the Eq. (15). This fitting (solid line in Fig. 7F) afforded values of T^* = 341.7 ± 2.4 K and E_{A} = 125.4±3.3 kcal mol^{-1}, which are in satisfactory agreement with the values obtained from DSC and CD experiments (see above).

4. Conclusions

Generally speaking, the origin of high stability in proteins does not result from a single mechanism but rather from the combination of several factors, such as increases of the number of ion pairs and hydrogen bonds, the core of hydrophobicity, packing density, the oligomerization of several subunits, glycosylation, and an entropic effect [48]. It is clear that a detailed study of the contribution of each factor to the unusually high stability of RPTP is required, but the results presented in this work together with their comparison with those reported for other plant peroxidases, allow us to conclude that the high stability of RPTP stems from its dimer structure. In fact, the overall folding and the organization of the secondary structure of all heme peroxidases from plants are conserved [49]. The structure of these proteins is formed by 10-12 α-helices (40-50%), linked by loops and turns, while β-structures are essentially absent or are only a minor component [43], and this is also the case of RPTP. All class III peroxidases have four conserved cysteine bridges [49] and about 40 basic and acidic amino acids. Like most secreted enzymes, plant peroxidases are glycoproteins with significant carbohydrate contents, and RPTP is no exception. It is glycosylated in approximately 24% of the molecular mass, and glycans are known to be heterogeneous (our own unpublished data). Moreover, the importance of glycosylation for the conformational stability of proteins is still unclear. Comparative studies of glycosylated and non-glycosylated proteins reported so far do not allow general conclusions to be drawn. Glycosylation may lead to a minor increase in the conformational stability of about ΔG = 0-1 kcal mol^{-1} and an increase in thermostability of about 0-2 °C [50]. Thus, as noted above, only the dimerization of RPTP differentiates this enzyme from other plant peroxidases, and this is probably why it is so stable and so promising for biotechnological applications.

Acknowledgments

This work was partially supported by the Programa de Acciones Integradas de Investigación Cientifica y Tecnológica (2006-2007) and by projects SA-06-00-0 ITACYL-Universidad de Salamanca and SA 129A07 (Junta de Castilla y León) and BFU2004-01432 (Ministerio de Educación y Ciencia) Spain. L.S.Z and O. G. are fellowship holders from the Junta de Castilla y León, Spain (Ref. EDU/1490/2003) and from the Fundação para a Ciência e a Tecnologia, Portugal (Ref. SFRH/BPD/28380/2006), respectively. D.G.P. was recipient of a Marie Curie Intra-European Fellowship from the European Commission (FP6).

References

1. C. Penel, T. Gaspar, H. Greppin, Plant Peroxidases 1980-90. Topics and Detailed Literature on Molecular, Biochemical, and Physiological Aspects. University of Geneva, Switzerland 1992.
2. K.G. Welinder, Superfamily of plant, fungal and bacterial peroxidases, Curr. Opin. Struct. Biol. 2 (1992) 388-393.
3. H.B. Dunford, Heme peroxidases. Wiley-Vch, New York, USA 1999.
4. J.S. Dordick, M.A. Marletta, A.M. Klibanov, Polymerization of phenols catalyzed by peroxidase in non-aqueous media, Biotechnol. Bioeng. 30 (1987) 31-36.
5. J.A. Akkara, K.J. Senecal, D.L. Kaplan, Synthesis and Characterization of polymers produced by horseradish peroxidase in dioxane, J. Polym. Sci: Part A: Polymer Chemistry 29 (1991) 1561-1574.
6. Q.R. Thompson, Peroxidase-based colorimetric determination of L-ascorbic acid, Anal. Chem. 59 (1987) 1119-1121.
7. Z. Weng, M. Hendrickx, G. Maesmans, P. Tobback, Immobilized peroxidase: a potential bioindicator for evaluation of thermal processes, J. Food Sci. 56 (1991) 567-570.
8. D. Arseguel, M. Baboulène, Removal of phenol from coupling of talc and peroxidase. Application for depollution of waste water containing phenolic compounds, J. Chem. Technol. Biotechnol. 61 (1994) 331-335.
9. P.R. Adler, R. Arora, A. El Ghaouth, D.M. Glenn, J.M. Solar, Bioremediation of phenolic compounds from water with plant root surface peroxidases, J. Environ. Qual. 23 (1994) 1113-1117.

10. A.V. Caramyshev, E.G. Evtushenko, V.F. Ivanov, A. Ros Barceló, M.G. Roig, V.L. Shnyrov, R.B. van Huystee, I.N. Kurochkim, A.K. Vorobiev, I.Y. Sakharov, Synthesis of conducting polyelectrolyte complexes of polyaniline and poly(2-acrylamido-3-methyl-1-propanesulfonic acid) catalyzed by pH-stable palm tree peroxidase, Biomacromolecules 6 (2005) 1360-1306.
11. A.G. MacDiarmid, Synthetic metals: a novel role for organic polymers, Synthetic Metals 125 (2001) 11-22.
12. E. Shoji, M.S. Freund, Potentiometric sensors based on the inductive effect on the pK(a) of poly(aniline): a nonenzymatic glucose sensor, J. Am. Chem. Soc. 123 (2001) 3383-3384.
13. W. Liu, J. Kumar, S. Treipathy, K.J. Senecal, L. Samuelson, Enzymatically synthesized conducting polyaniline, J. Am. Chem. Soc. 121 (1999) 71-78.
14. I.Y. Sakharov, M.K. Vesga, I.Y. Galaev, I.V. Sakharova, O.Y. Pletjushkina, Peroxidase from leaves of royal palm tree *Roystonea regia:* purification and some properties, Plant Sci. 161 (2001) 853-860.
15. L. Watanabe, A.S. Nascimento, L.S. Zamorano, V.L. Shnyrov, I. Polikarpov, Purification, crystallization and preliminary X-ray diffraction analysis of royal palm tree (*Roystonea regia*) peroxidase, Acta Cryst. F63 (2007) 780-783.
16. I.Y. Sakharov, M.K. Vesga Blanco, I.V. Sakharova, Substrate specificity of african oil palm tree peroxidase, Biochemistry (Moscow) 67 (2002) 1043-1047.
17. G. Fairbanks, T. Steck, D.F.N. Wallach, Electrophoretic analysis of the major polypeptides of the human erythrocyte membrane, Biochemistry 10 (1971) 2606-2617.

18. A. Lindgren, T. Ruzgas, L. Gorton, E. Csöregi, G.B. Ardila, I.Y. Sakharov, I.G. Gazaryan, Biosensors based on novel peroxidases with improved properties in direct and mediated electron transfer, Biosens. Bioelectron. 15 (2000) 491-497.

19. J. Vistica, J. Dam, A. Balbo, E. Yikilmaz, R.A. Mariuzza, T.A. Rouault, P. Schuck, Sedimentation equilibrium analysis of protein interactions with global implicit mass conservation constraints and systematic noise decomposition, Anal. Biochem. 326 (2004) 234-256.

20. P. Schuck, Size-distribution analysis of macromolecules by sedimentation velocity ultracentrifugation and Lamm equation modeling, Biophys. J. 78 (2000) 1606-1619.

21. L.S. Zamorano, D.G. Pina, F. Gavilanes, M.G. Roig, I.Y. Sakharov, A.P. Jadan, R.B. van Huystee, E. Villar, V.L. Shnyrov, Two-state irreversible thermal denaturation of anionic peanut (*Arachis hypogaea* L.) peroxidase, Thermochim. Acta 417 (2004) 67-73.

22. D.G. Pina, J. Gómez, P. England, C.T. Craescu, L. Johannes, V.L. Shnyrov, Characterization of the non-native trifluoroethanol-induced intermediate conformational state of the Shiga toxin B-subunit, Biochimie 88 (2006) 1199-1207.

23. B.I. Kurganov, A.E. Lyubarev, J.M. Sanchez-Ruiz, V.L. Shnyrov, Analysis of differential scanning calorimetry data for proteins. Criteria of validity of one-step mechanism of irreversible protein denaturation, Biophys. Chem. 69 (1997) 125-135.

24. J.W. Tams, K.G. Welinder, Unfolding and refolding of *Coprinus cinereus* peroxidase at high pH, in urea, and at high temperature. Effect of organic and ionic additives on these processes, Biochemistry 35 (1996) 7573-7579.

25. D.G. Pina A.V. Shnyrova, F. Gavilanes, A. Rodríguez, F. Leal, M.G. Roig, I.Y. Sakharov, G.G. Zhadan, E. Villar, V.L. Shnyrov, Thermally induced conformational changes in horseradish peroxidase, Eur. J. Biochem. 268 (2001) 120-126.
26. I.Y. Sakharov, I.V. Sakharova, Extremely high stability of African oil palm tree peroxidase, Biochim. Biophys. Acta 1598 (2002) 108-114.
27. E.A. Permyakov, Luminescent spectroscopy of proteins. Boca Raton: CRC Press, 1993.
28. S.P. Manly, K.S. Matthews, J.M. Sturtevant, Thermal denaturation of the core protein of lac repressor, Biochemistry 24 (1985) 3842-3846.
29. E. Freire, Statistical thermodynamic analysis of the heat capacity function associated with protein folding-unfolding transitions, Comm. Mol. Cell. Biophys. 6 (1989) 123-140.
30. K. Takahashi, J.M. Sturtevant, Thermal denaturation of streptomyces subtilisin inhibitor, subtilisin BPN', and the inhibitor-subtilisin complex, Biochemistry 20 (1981) 6185-6190.
31. E. Freire, W.W. van Osdol, O.L. Mayorga, J.M. Sanchez-Ruiz, Calorimetrically determined dynamics of complex unfolding transitions in proteins, Annu. Rev. Biophys. Biophys. Chem. 19 (1990) 159-188.
32. J.M. Sanchez-Ruiz, Theoretical analysis of Lumry-Eyring models in differential scanning calorimetry, Biophys. J. 61 (1992) 921-935.
33. R. Lumry, H. Eyring, Conformation Changes of Proteins, J. Phys. Chem. 58 (1954) 110-120.

34. A.E. Lyubarev, B.I. Kurganov, Modeling of irreversible thermal protein denaturation at varying temperature. I. The model involving two consecutive irreversible steps, Biochemistry (Moscow) 63 (1998) 434-440.

35. A.E. Lyubarev, B.I. Kurganov, Modeling of irreversible thermal protein denaturation at varying temperature. II. The complete kinetic model of Lumry and Eyring, Biochemistry (Moscow) 64 (1999) 832-838.

36. A. Rodríguez, D.G. Pina, B. Yélamos, B., J.J. Castillo Leon, G.G. Zhadan, E. Villar, F. Gavilanes, M.G. Roig, I.Y. Sakharov, V.L. Shnyrov, Thermal stability of peroxidase from the african oil palm tree *Elaeis guineensis*, Eur. J. Biochem. 269 (2002) 2584-2590.

37. A.T. Lu, J.R. Whitaker, Some factors affecting rates of heat inactivation and reactivation of horseradish peroxidase, J. Food Sci. 36 (1974) 1173-1178.

38. J.P. McEldon, J.S. Dordick, Unusual thermal stability of soybean peroxidase, Biotechnol. Prog. 12 (1996) 555-558.

39. P.L. Privalov, S.A. Potekhin, Scanning microcalorimetry in studying temperature-induced changes in proteins, Methods Enzimol. 131 (1986) 4-51.

40. W.J. Becktel, J.A. Schellman, Protein stability curves, Biopolymers 26 (1987) 1859-1877.

41. M. Sawano, H. Yamamoto, K. Ogasahara, S. Kidokoro, S. Katoh, T. Ohnuma, E. Katoh, S. Yokoyama, K. Yutani, K. Thermodynamic basis for the stabilities of three CutA1s from *Pyrococcus horikoshii*, *Thermus thermophilus*, and *Oryza sativa*, with unusually high denaturation temperatures, Biochemistry 47 (2008) 721-730.

42. N. Sreerama, S.Y. Venyaminov, R.W. Woody, Estimation of the number of alpha-helical and beta-strand segments in proteins using circular dichroism spectroscopy, Protein Sci. 8 (1999) 370-380.
43. L. Banci, Structural properties of peroxidases, J. Biotechnol. 53 (1997) 253-263.
44. S.Y. Venyaminov, J.T. Yang, Determination of protein secondary structure, in: Circular Dichroism and the Conformational Analysis of Biomolecules (G.D. Fasman, ed) pp. 69-107, Plenum Press, New York, 1996.
45. C.N. Pace, Determination and analysis of urea and guanidine hydrochloride denaturation curves, Methods Enzymol. 131 (1986) 266-280.
46. J.K. Myers, C.N. Pace, J.M. Scholtz, Denaturant m values and heat capacity changes: relation to changes in accessible surface areas of protein unfolding, Protein Sci. 4 (1995) 2138-2148.
47. B.C. Hill, P.M. Horowitz, N.C. Robinson, Detection, characterization, and quenching of the intrinsic fluorescence of bovine heart cytochrome c oxidase, Biochemistry 25 (1986) 2287-2292.
48. G.A. Petsko, Structural basis of thermostability in hyperthermophilic proteins, or "there's more than one way to skin a cat", Methods Enzymol. 334 (2001) 469-478.
49. K.G. Welinder, M. Gajhede, Structure and evolution of peroxidases, in: Plant Peroxidases Biochemistry and Physiology pp. 35-42, University of Copenhagen and University of Geneva, Geneva, Switzerland, 1993.
50. W. Pfeil, The influence of glycosylation on the thermal stability of ribonuclease, Thermochim. Acta 382 (2002) 169-174.

Figure legends

Fig. 1. pH-dependence of enzymatic activity (A) and fluorescence parameters (B) of RPTP at 25 °C. Measurements were performed in 10 mM universal buffer (CH_3COOH, H_3PO_4, H_3BO_3-NaOH) with a protein concentration of ca. 10 μM. Activity was measured towards guaiacol. The excitation wavelength was 296 nm. Open circles in (B) represent fluorescence intensity (arbitrary units) at 350 nm, which is proportional to the fluorescence quantum yield, and closed circles correspond to the position of the maximum of the fluorescence spectrum λ_{max}.

Fig. 2. (A) Sedimentation velocity and equilibrium experiments. (A) Normalized molar distribution of RPTP at 25 °C in: 20 mM HEPES, pH 7.0, for a protein concentration of 0.8 mg mL^{-1} (continuous line) and 2.5 mg mL^{-1} (dashed line) and 20 mM citrate buffer, pH 3.0, for a protein concentration of 0.8 mg mL^{-1} (dotted line) and 2.5 mg mL^{-1} (dashed-dotted line) obtained by sedimentation velocity measurements. (B) The sedimentation equilibrium experiment was performed at a protein concentration of 1.0 mg mL^{-1} in 20 mM citrate buffer, pH 3.0, containing 6 M Gu-HCl at 25 °C. The solid line drawn through the data points was obtained by fitting for a single ideal species. The residuals (difference between the experimental results and the fitted data) are shown in the bottom panel.

Fig. 3. Typical excess molar heat capacity curves of RPTP in 20 mM HEPES buffer at pH 7.0. (A) Reversibility of heat denaturation of RPTP at pH 7.0. DSC curves were obtained for protein with a concentration of 18 μM at a scan rate of 60.1 K h^{-1}. The dashed line is the second DSC run performed immediately after cooling of the first run

(continuous line), which was performed up to 100 °C. The recovery area of excess heat capacity was nearly 80%. (B) Excess molar heat capacity curves of RPTP obtained at a scan rate of 60.8 K h^{-1} for protein concentrations of 12.7 μM (open circles) and 50 μM (closed circles). The solid lines represent theoretical curves generated with the two-state folding/unfolding coupled with oligomerization model and the best set of fitting parameters obtained by non-linear least squares optimization.

Fig. 4: Plot of the logarithm of the monomer molar RPTP concentration vs. T_m^{-1} at pH 7.0. T_m is the absolute value of the temperature at which the excess heat capacity (see Fig. 3) is maximum. The line represents the linear least-squares fit of the experimental data.

Fig. 5: Temperature dependence of the excess molar heat capacity of RPTP at scan rates of 30.1 K h^{-1} (squares), 60.2 K h^{-1} (circles) and 88.2 K h^{-1} (triangles) in 20 mM citrate buffer, pH 3.0. Solid lines represent the best fit to each experimental curve using Eq. (7). The protein concentration was 18 μM.

Fig. 6. Temperature functions of the unfolding free energy for RPTP at pH 7.0 (solid line) and pH 3.0 (dashed line). Circles represent the effective free energy value at pH 7.0 and 25 ^{o}C, obtained from the Gdn-HCl denaturation curve at a protein concentration of 16 μM; close to the protein concentration in the DSC experiments. The temperature dependence of ΔG for RPTP at pH 3.0 was calculated with thermodynamic parameters (see Table 2) obtained by extrapolating the experimental data to an infinite heating rate which should be close to the real values [39].

Fig. 7. Gdn-HCl and thermally induced denaturation of RPTP studied by optical spectroscopy. (A) Far-UV CD spectra of RPTP at pH 7.0 without (open circles) and with 7.1 M (closed circles) Gdn-HCl. The spectra were measured at 25 ^{o}C with a fixed protein concentration of 10 μM. The solid line through the open circles is the best fit of the experimental data with the CDSSTR program, using SP43 as a reference set. (B) Fractional degree of unfolding of RPTP as a function of the Gdn-HCl concentration monitored by the change in ellipticity at 222 nm. The inset shows the differences in free energy between the folded and denatured conformations of RPTP (symbols) calculated from measurements of the changes in the ellipticity with increases in the Gdn-HCl concentration in the transition region using Eq. (13). The straight line is the result of the least squares fitting of the data to Eq. (14). (C) Far-UV spectra at pH 3.0 of intact RPTP at 25 ºC (open circles) and thermally denatured RPTP at 80 ºC (closed circles). The solid lines through the symbols are the best fits to the experimental data with the CDSSTR program, using SP43 for the intact and SDP48 for denatured protein as reference sets. (D) Fractional degree of thermal unfolding of RPTP as a function of temperature, at pH 3.0, monitored by the changes in ellipticity at 222 nm, obtained upon heating at a constant scan rate of 60.1 K h^{-1}. The solid line represents the theoretical curve resulting from fitting the experimental data to the two-state irreversible model using Eq. (15). (E) Fluorescence spectra of intact -at 25 ºC (solid line)- and thermally denatured -at 80 ºC (dashed line)- RPTP at pH 3.0. The excitation wavelength was 296 nm. (F) Fractional degree of thermal unfolding of RPTP as a function of temperature monitored by the changes in fluorescence intensity at 360 nm at pH 3.0, obtained upon heating at a constant scan rate of 96 K h^{-1}. The solid line represents the best fit obtained using Eq. (15).

Figure1
Click here to download high resolution image

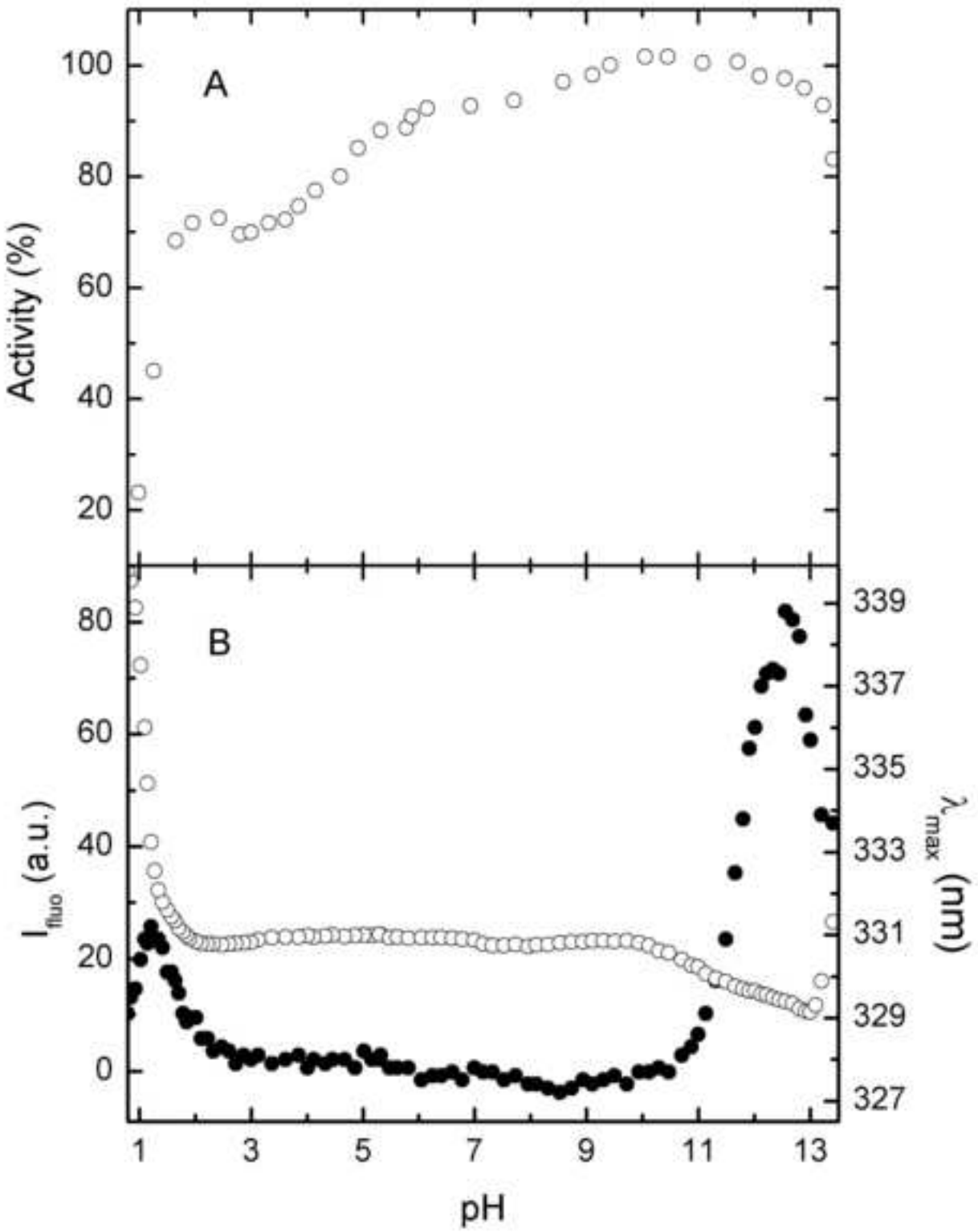

Figure 1

Figure2
Click here to download high resolution image

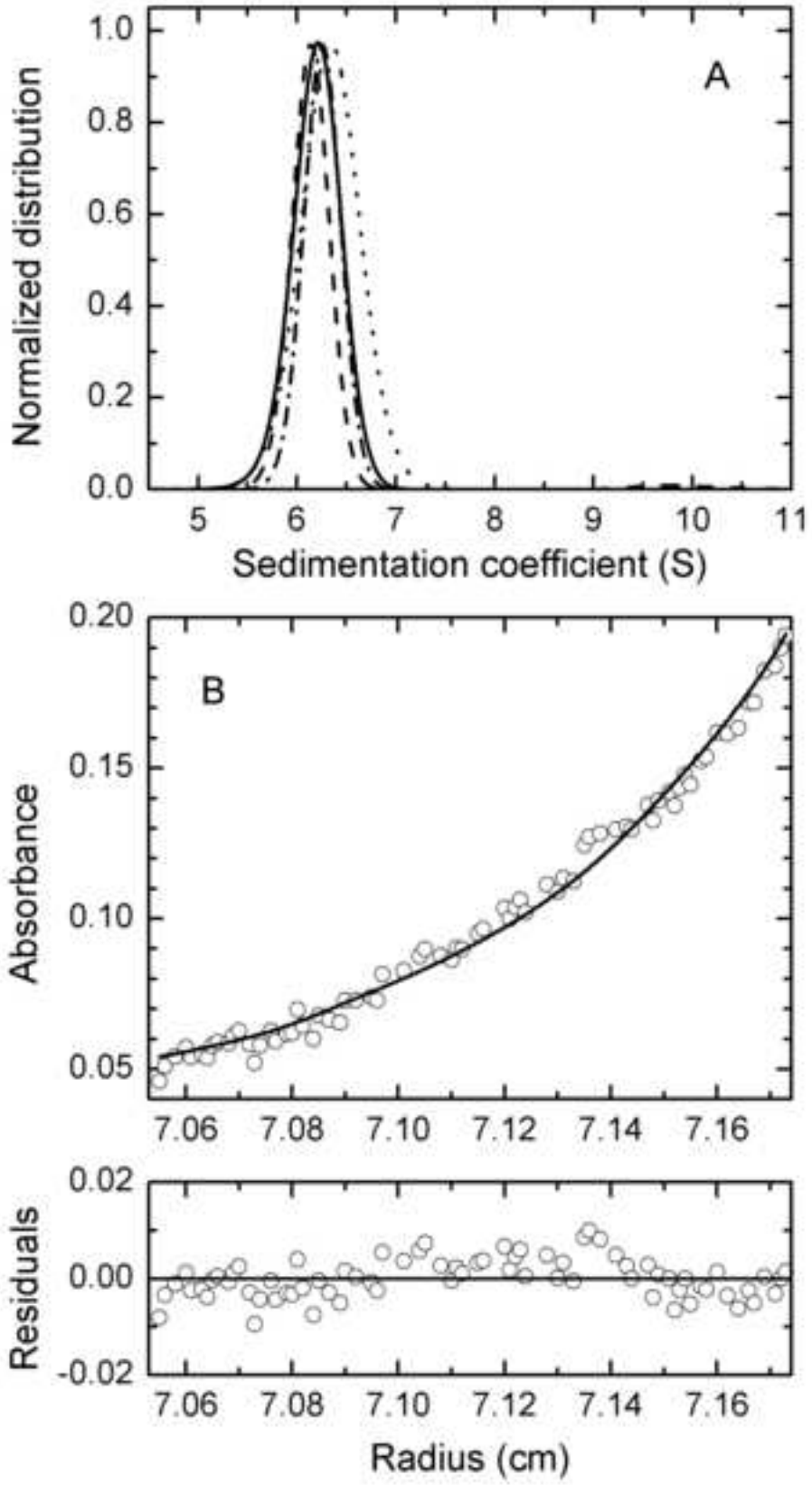

Figure 2

Figure3
Click here to download high resolution image

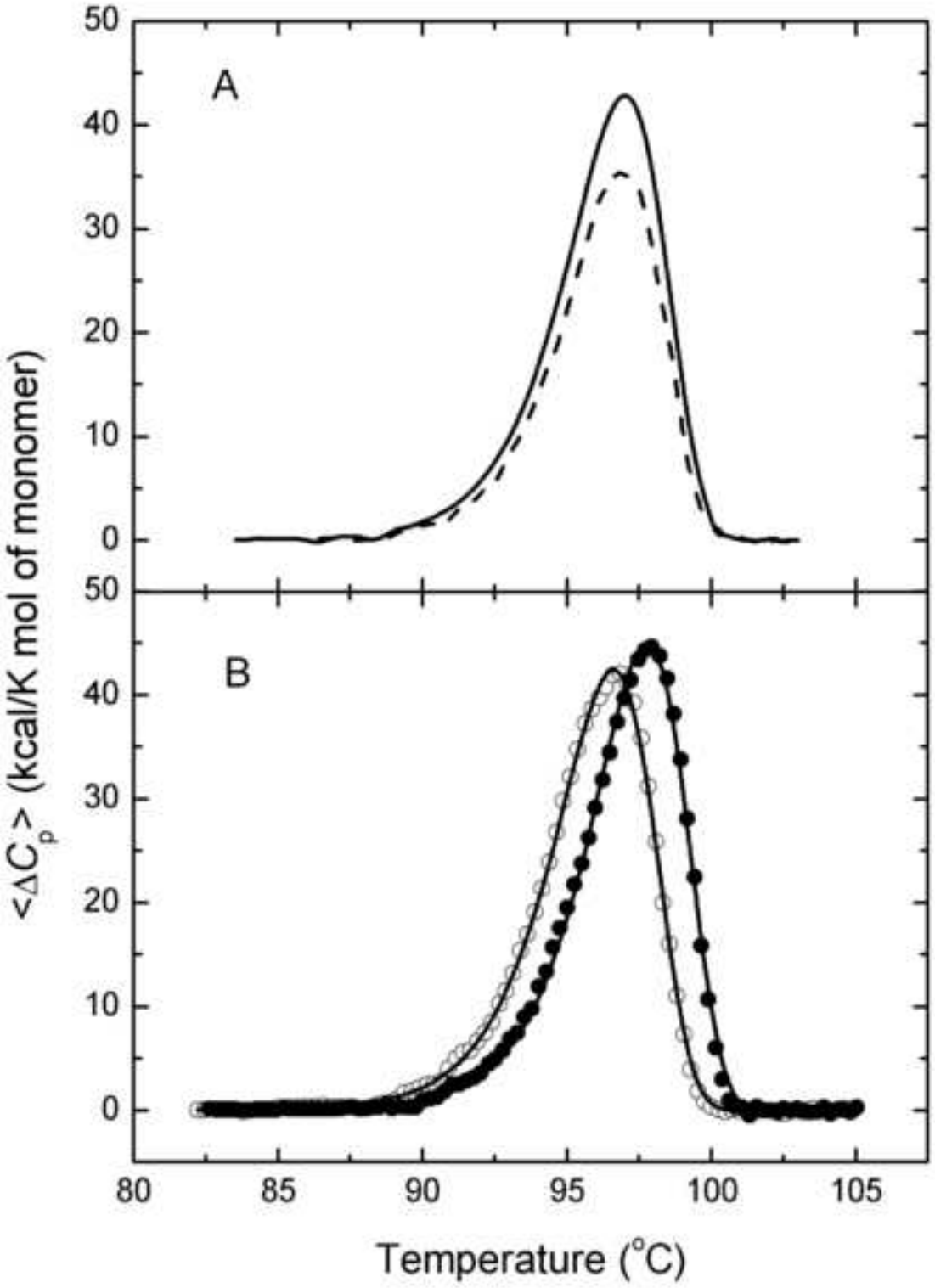

Figure 3

Figure4
Click here to download high resolution image

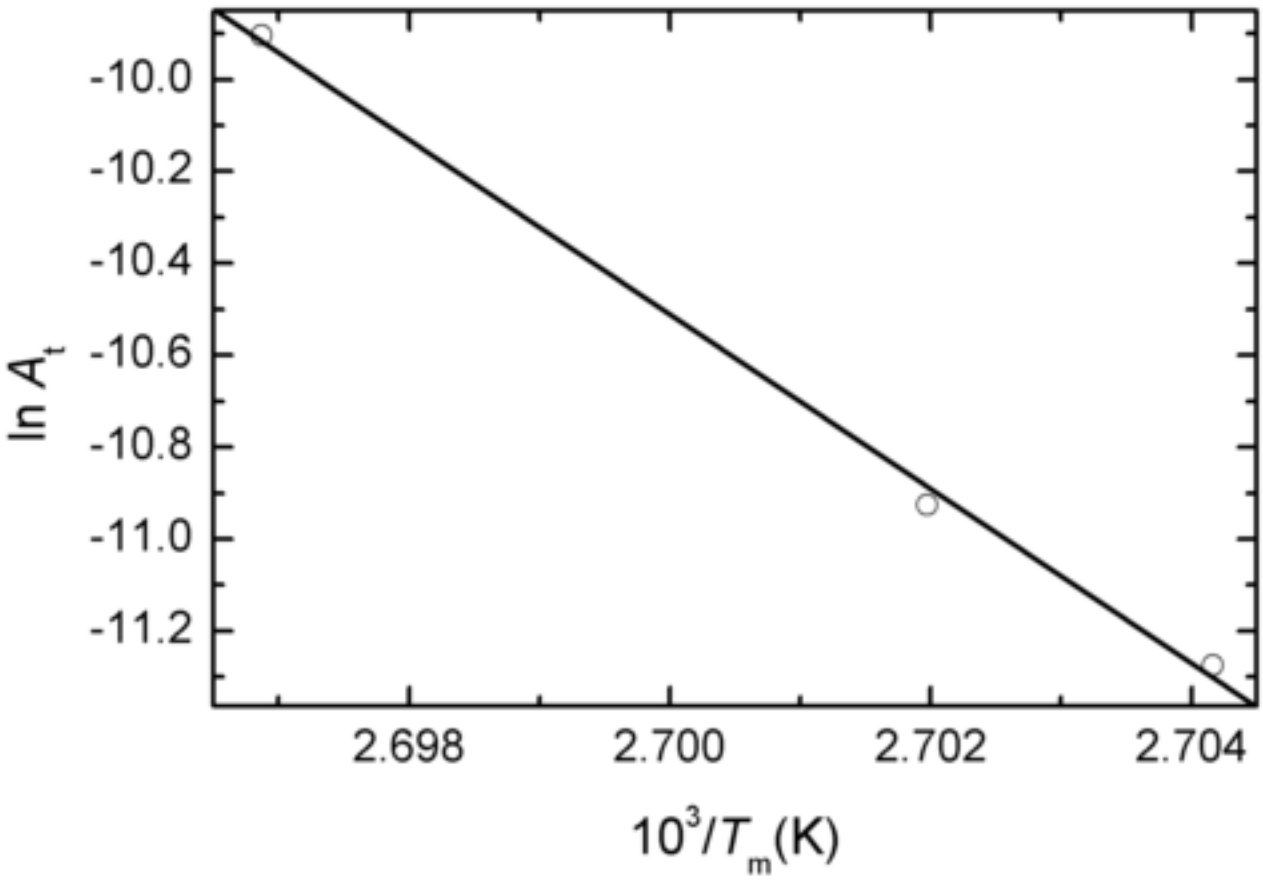

Figure 4

Figure5
Click here to download high resolution image

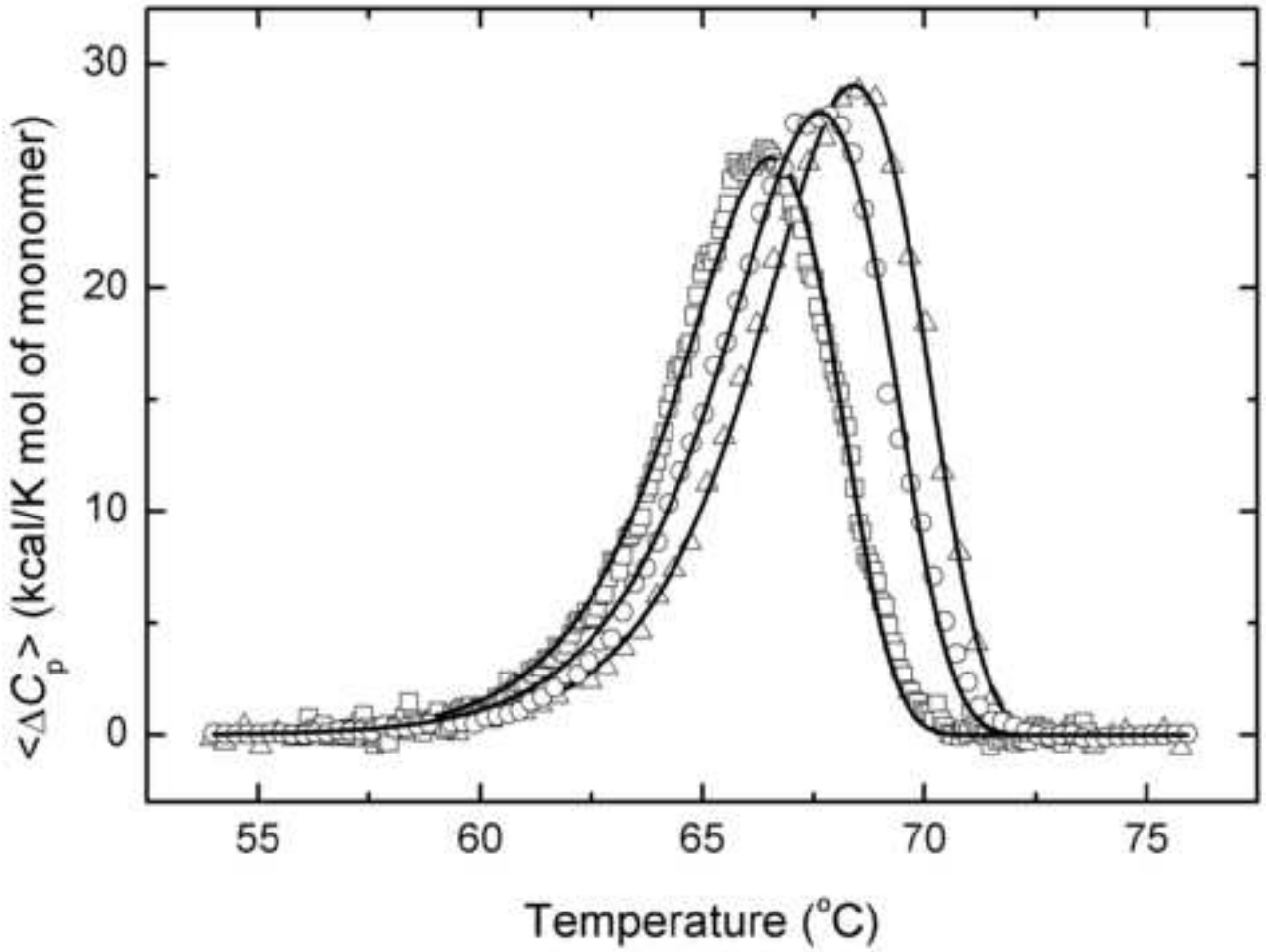

Figure 5

Figure6
Click here to download high resolution image

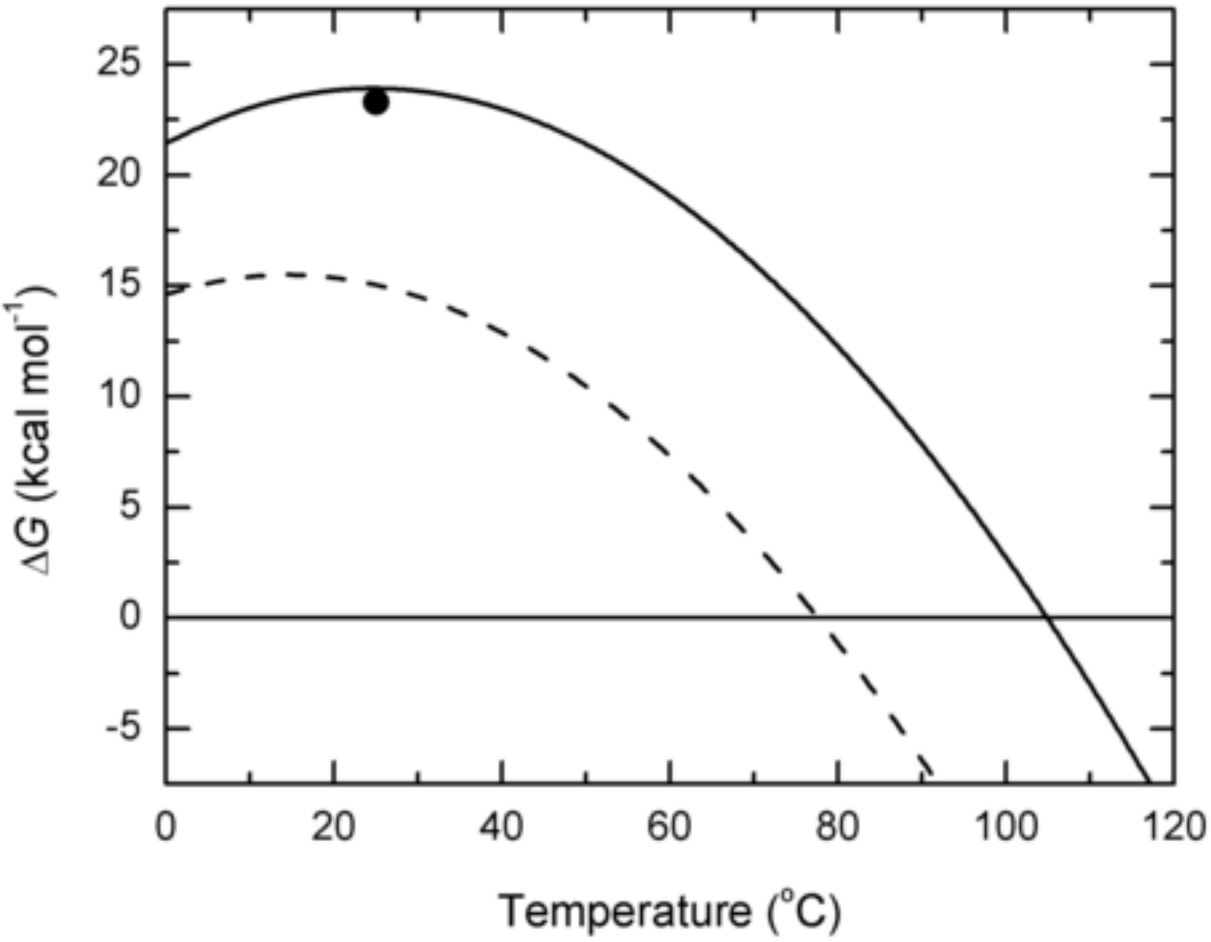

Figure 6

Figure7

Click here to download high resolution image

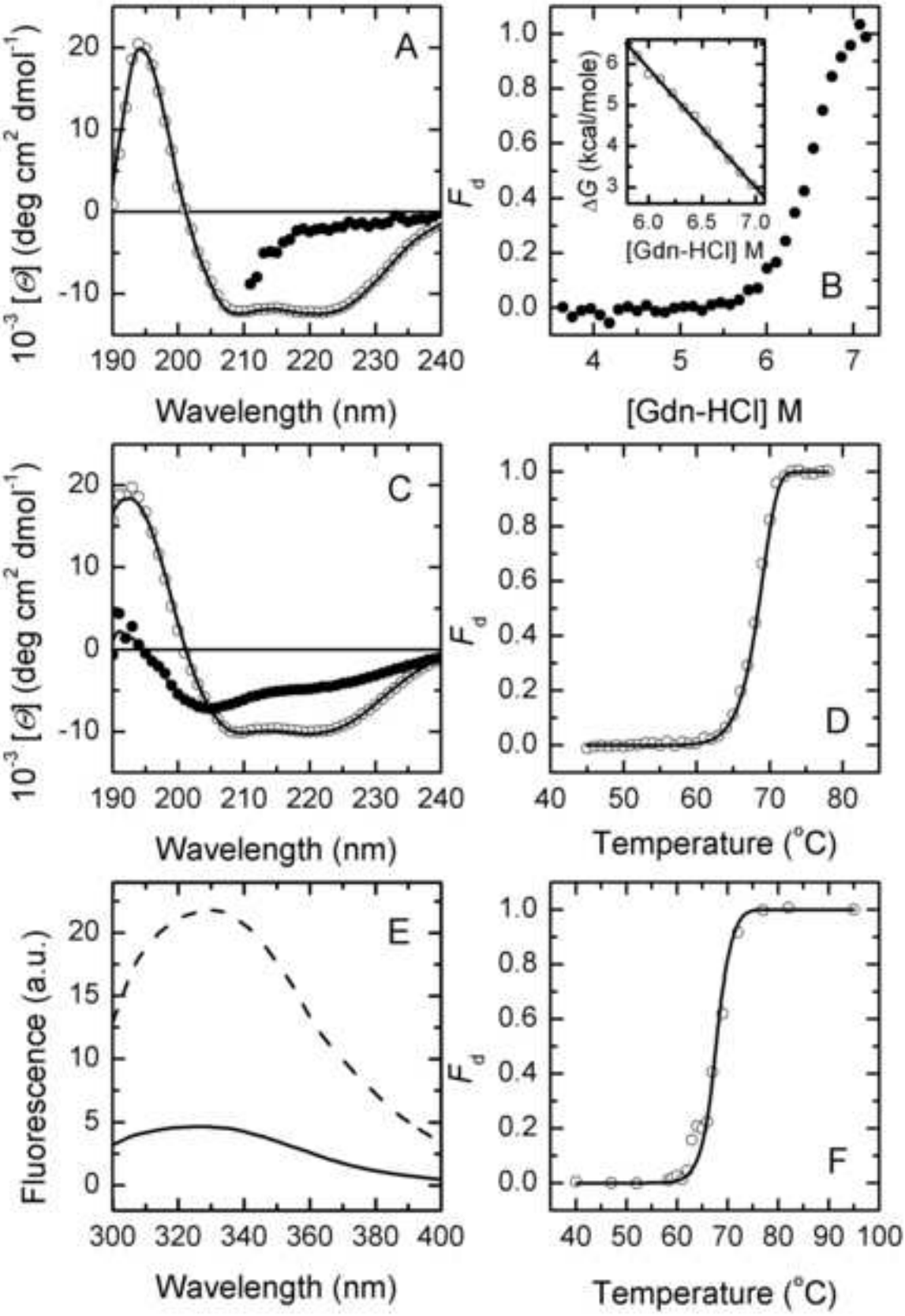

Figure 7

Tables

Table 1

Apparent molecular weights of RPTP at several pH values and protein concentrations at 25 °C

pH	Protein concentration ($mg\ mL^{-1}$)	Sedimentation coefficient (S)	MW
7.0	1.0	6.19 ± 0.25	87530 ± 5250
7.0	2.5	6.13 ± 0.19	90140 ± 4100
		9.94 ± 0.47 (2nd species)	188100 ± 10300
3.0	1.0	6.34 ± 0.31	88250 ± 6500
3.0	2.5	6.26 ± 0.20	88040 ± 3780

Table 2

Thermodynamic parameters for the thermal denaturation of RPTP

[RPTP] (μM)	pH	T_m (°C)	$T_{1/2}$ (°C)	T_o (°C)	$\Delta H(T_m)$ (kcal mol^{-1})	T_s (°C)	$\Delta G(T_s)$ (kcal mol^{-1})
12.7	7.0	96.7	95.9	104.6	196.2	24.1	23.9
18.0	7.0	97.0	96.2	104.8	197.0	24.3	24.0
50.0	7.0	97.7	97.0	104.7	198.8	24.2	23.9
18.0	3.0	69.0	68.3	77.6	144.5	13.6	15.5

The standard deviation for T_m and $T_{1/2}$ values is ± 0.2 K; the enthalpy of the denaturation was determined with a standard deviation of ± 5%; T_o is the temperature value at which $\Delta G^o(T) = 0$. T_s, the temperature of maximum stability, was calculated with the equation: $T_s = \exp[-\Delta H(T_o)/(T_o \Delta C_p)]$ [40] and ΔC_p = 2.4 ± 0.1 kcal K^{-1} mol^{-1} was calculated from the slope of the plot of the temperature-dependence of enthalpy by varying pH from 3 to 9.

Table 3

Arrhenius equation parameter estimates for the two-state irreversible model of the thermal denaturation of RPTP (protein concentration of 18 μM) at pH 3.0

Parameter	Temperature scan rate (K h^{-1})			Global
	30.1	60.2	88.2	fitting
ΔH (kcal mol^{-1})	121.8 ± 1.9	140.0 ± 1.2	144.2 ± 1.2	
T^* (K)	341.9 ± 0.2	342.0 ± 0.1	342.0 ± 0.1	342.0 ± 0.2
E_A (kcal mol^{-1})	130.5 ± 0.6	128.8 ± 0.5	127.4 ± 0.5	129.8 ± 0.8
r	0.9978	0.9980	0.9984	0.9969

The correlation coefficient (r) was calculated as $r = \sqrt{1 - \sum_{i=1}^{n}\left(y_i - y_i^{calc}\right)^2 / \sum_{i=1}^{n}\left(y_i - y_i^{m}\right)^2}$, where y_i and y_i^{calc} are respectively the experimental and calculated values of C_p^{ex}; y_i^m is the mean of the experimental values of C_p^{ex}, and n is the number of points.

Table 4

Secondary structure elements (%) determined from analysis of the CD spectra for RPTP

Protein	α-Helix			β-Strand			β-Turn	Unordered
	Regular	Distorted	Total	Regular	Distorted	Total		
Intact, pH 7.0	28	26	54	3	4	7	24	15
Intact, pH 3.0	22	19	41	7	5	12	20	27
Denatured, pH 3.0	3	5	8	13	7	20	16	56